3rd European supercritical CO2 Conference
September 19-20, 2019, Paris, France

2019-sCO2.eu-118

A SYSTEMATIC COMPARISON OF SUPERCRITICAL CO_2 BRAYTON CYCLE LAYOUTS FOR CONCENTRATED SOLAR POWER WITH A FOCUS ON THERMAL ENERGY STORAGE UTILIZATION

Jinyi Zhang*
EDF R&D China
Beijing, China
Email: Jinyi.zhang@edf.fr

Yann Le Moullec
EDF R&D China
Beijing, China

ABSTRACT

Supercritical CO_2 cycle, due to its potential to reach high thermal efficiency and high flexibility, is a promising approach to increase the competitiveness of concentrated solar power. By taking into account thermal energy storage utilization, this paper provides a meaningful comparison of different supercritical CO_2 cycles for application in concentrated solar power. Regenerative, recompression, pre-compression and partial cooling cycles are considered as four fundamental cycles. By combining these fundamental cycles with intercooling, preheating and reheating, it results in a wide range of cycle candidates for comparison and analysis. Each cycle is modeled and optimized with the objective to maximize the specific power output for different thermal energy storage utilization. The results show that, with a high thermal energy storage utilization, in order to maximize the cycle efficiency, it is not optimal for most of the studied cycle to reach its upper limit of temperature. Besides, with the thermal storage utilization as a constraint for optimization, intercooling, preheating and reheating show different efficiency enhancement behavior on different region of thermal energy storage utilization.

INTRODUCTION

In recent years, facing the worldwide environmental challenge and the scarcity of fossil fuels in some regions of the world, renewable energy is gaining more and more importance in the development portfolio of energy industry. Solar and wind energy are two major renewable energy solutions which attract most of the attentions, however, the highly uncontrollable variability of solar irradiation and wind bring huge challenges for the electric power grid to match the instantaneous energy demand and production. As a result, the renewables are suffering serious curtailment, e.g. in 2016, the curtailment of wind and solar PV energy reached 57.3 TWh in China [1]. In addition, the highly uncontrollable variability of solar irradiation and wind also limits the highest share of renewable energy that can be integrated into the power system in the future. Concentrated solar power (CSP), which can reach a high solar energy utilization efficiency and operate with low-cost thermal energy storage (TES), e.g. the commercially utilized molten salt, namely Solar Salt (60 wt% $NaNO_3$ and 40 wt% KNO_3), is a grid-friendly renewable solution. Because CSP, if equipped with enough TES, is able to completely decouple the solar-thermal and thermal-electricity conversions, achieving continuous production and regulating the power output depending on the grid demand, regardless of the weather conditions.

However, CSP's high cost, 120 $/MWh in average in 2020 reported by International Renewable Energy Agency (IRENA), makes it difficult for long-term deployment. In order to increase its competitiveness compared to other renewable solutions with storage, in addition to the efforts done to reduce the capital cost, there are two main technology development paths: one is to increase the solar-thermal efficiency by optimizing solar collector efficiency, the other is to increase the thermal-electricity efficiency by increasing the thermal storage temperature or the power generation cycle efficiency. Supercritical CO_2 (SCO_2) power generation cycle is identified as a promising technology with high potential in the second path to increase the thermal-electric efficiency and reduce the capital cost due to simpler layout and more compact turbo-machinery [2–6].

Besides, CO_2 also exhibits many attracting characteristics as a heat transfer fluid [7–9]: It is abundant, inexpensive, non-toxic and it has a easily-achievable critical point (30.98 ℃, 7.38 MPa). It also shows a good thermal stability up to 1500 ℃ and no freezing problem down to -55 ℃. Gas Brayton cycle operating with SCO_2 benefits from the real gas behavior of CO_2 in the vicinity of the Andrews curve, which leads to the reduction of specific volume and therefore of the compression work in the cycle. More reduction of compression work is achieved when CO_2 is compressed closer to its critical point, as the fluid becomes more incompressible. This mechanical effect, i.e. the significant reduction of compression work, results in a significant thermal efficiency improvement of SCO_2 Brayton

* corresponding author(s)

DOI: 10.17185/duepublico/48879

cycle compared to other working fluid for Brayton cycle, e.g. helium or air [10]. As the SCO_2 cycle operates with high pressure and small pressure ratio, the fluid remains dense throughout the entire system, as a result, the volume of turbo-machineries is significantly reduced, ~90% smaller than water steam turbine [10]. The fact that replacing water by CO_2 in the power block simplifies significantly the operation of CSP plants which are mostly located in the droughty areas.

Feher is one of the first authors who proposed CO_2 as a heat transfer fluid for power generation cycle and pointed out the pinch problems of recuperator in a regenerative cycle [7]. Anglino performed one of the earliest and the most detailed investigation of SCO_2 cycles and introduced novel cycle configurations such as recompression, pre-compression and partial cooling, to overcome the internal irreversibility problem in the recuperator then to improve the cycle performance [8,11,12]. Dostal, based mainly on the cycle configurations proposed by Anglino, further introduced intercooling and reheating, carried out a comprehensive study on SCO_2 cycles for application to advanced nuclear reactors and concluded that recompression cycle yielded the highest efficiency while remaining simple.

With the development of CSP, more and more studies have been focusing on the integration of CSP and SCO_2 cycle. Yamaguchi proposed SCO_2 Rankine cycle for solar thermal power generation and built an experimental loop to study the characteristics of SCO_2 cycle coupled with solar energy [13–15], but no cycle selection or optimization has been done. Turchi did some dedicated study on SCO_2 cycles for CSP [2–6,16] and concluded that partial cooling cycle outperformed the recompression cycle and pointed out that the importance of larger temperature differential across the primary heat exchanger for more cost efficient thermal energy storage (TES) systems and possible more thermally efficient receivers [16]. Many studies have also been done for the application of SCO2 cycles in coal-fired power (CFP) [17–19] and waste heat recovery (WHR) [20–22]. Because CFP needs to recover as much as possible the combustion heat to maximize the boiler efficiency and WHR needs to recover the low-grade heat to maximize the net power output from the bottoming cycle, SCO_2 cycles with preheating are firstly proposed for these applications, in order to achieve a larger temperature differential utilization of heat source [17,21]

More studies are also found in recent years to analyze different SCO_2 cycles for application in CSP [23–29]. However, most of the current cycle studies for CSP have been focusing on the comparison or optimization of cycle in terms of thermal efficiency or overall plant efficiency, which resulted in poor utilization of thermal storage potential. However, for CSP plant, due to the fact that TES system represents ~20% of the total plant investment, it requires that the potential of thermal storage medium should be efficiently exploited in order to reach a more cost-efficient design of TES system. In the meantime, the cycle thermal efficiency should be kept as high as possible to minimize the levelized cost of electricity (LCOE). In order to take these two factors together into account, the electric power generated from a specific amount of thermal storage, which is equivalent to the product of thermal storage utilization ratio and cycle thermal efficiency, is selected as a cycle performance criterion in this study. Besides, thermal storage utilization ratio, as a function of cold-side temperature and hot-side temperature, is the juncture among the three main subsystems of CSP, i.e. solar field, TES and power block. It influences directly the thermal-electrical efficiency of power block, solar-thermal efficiency and the size of TES system. Therefore, it is an important indicator for the integration of SCO_2 with CSP and a better understanding on its impact on the performance could provide a clearer guideline on the selection of SCO_2 cycle for application in CSP.

This paper aims to provide a meaningful comparison of different SCO2 cycles for application in CSP with Solar Salt, by taking into account the TES utilization. Regenerative, recompression, pre-compression and partial cooling cycle are considered as four fundamental cycles. By combining these fundamental cycles with several cycle characteristics such as intercooling, preheating and reheating, it results in a wide range of cycle candidates for comparison and analysis in this paper.

SCO_2 CYCLES

Regenerative (RG) cycle is the simplest cycle that is able to achieve an acceptable performance, but due to the pinch-point problem in the recuperator, its potential to reach a high thermal efficiency is limited. Most of the complex SCO_2 cycles are derived from RG cycle, therefore, it is considered as a reference for cycle analysis and comparison. Regenerative cycle with recompression, i.e. recompression (RC) cycle, solves the pinch-point problem by splitting part of the hot-side outlet flow of the recuperator. One part of the flow passes the cooler, the main compressor and recuperator, while the other part of flow enters directly into an auxiliary compressor. These two flows join later at the cold-side outlet of recuperator. As a result, RC cycle achieves higher thermal efficiency compared to RG cycle. Pre-compression (PC) cycle introduces another approach to reduce the effect of the pinch-point problem. It reduces the heat capacity difference between low-pressure and high-pressure flows by increasing the pressure of the low-pressure flow. Partial cooling (PartC) cycle is similar to RC cycle except that the recuperator hot-side outlet flow is cooled down and compressed to a higher pressure before splitting into two flows. These 4 cycles are the most fundamental SCO_2 cycles for analysis.

Besides, there are several cycle characteristics that can be combined with these fundamental cycles: (1) Intercooling (IC) between stages of compressor is a classical approach to reduce the compressor work then to improve cycle efficiency; (2) Pre-heating (PH) means to split a part of the recuperator cold-side outlet flow and make it heated by the low-grade heat of heat

Table 1
Fundamental SCO_2 cycles with their derivatives

Fundamental	+ IC	+ PH	+ RH
RG	RG-IC	RG-PH	RG-RH
RC	RC-IC	RC-PH	RC-RH
PC	PC-IC	PC-PH	PC-RH
PartC	PartC-IC	PartC-PH	PartC-RH

DOI: 10.17185/duepublico/48879

Table 2
Modelling hypotheses for performance preliminary assessment

Parameters	Unit	Value
Maximum molten salt temperature, T_{max}^{MS}	℃	565
Minimum molten salt temperature, T_{min}^{MS}	℃	290
Maximum pressure, p_{max}	MPa	25
Main compressor inlet temperature, T_{MCI}	℃	35
Pre-compressor inlet temperature, T_{PCI}	℃	35
Compressor isentropic efficiency, η_{cmp}	%	89
Turbine isentropic efficiency, η_{tb}	%	93
Molten salt/CO_2 heat exchanger minimum internal pinch, $\Delta T_{min}^{MS/CO2}$	℃	5
CO_2/CO_2 heat exchanger minimum internal pinch, $\Delta T_{min}^{CO2/CO2}$	℃	5
Molten salt /CO_2 heat exchanger pressure drop (CO_2 side), $\Delta p^{MS/CO2}$	MPa	0.1
CO_2 /CO_2 heat exchanger pressure drop, $\Delta p^{CO2/CO2}$	MPa	0.1

source in the pre-heater before entering into the next recuperator (if any) or the main heater. (3) Reheating (RH) between high-pressure and low-pressure turbine is another classical approach to improve the cycle efficiency. These four fundamental cycles combined with IC, PH and RH, result in sixteen cycles as shown in Table 1. All the cycle layouts are shown in Annex A.

DESIGN BOUNDARY CONDITIONS AND HYPOTHESIS

This paper aims to present the SCO_2 cycle study for the current high-temperature CSP technology, i.e. Solar Salt tower technology. Therefore, Solar Salt's physical property and operation temperature range 290 ℃ and 565 ℃ is used to define the TES system, which serves as the design boundary condition for power block since TES system is the only interface between solar field and power block. The key hypothesis for cycle modeling and calculation is listed in Table 2.

MODELING AND STUDY APPROACH

1. Equipment Model

All the equipment model used in the cycle performance analysis is zero-dimension model based on energy balance equation. For cycle analysis, three types of equipment are needed: turbine, compressor and heat exchanger. Table 3shows the governing equations used for them.

Table 3
Governing equations for main equipment

Equipment	Governing equations
Turbine	$W = \dot{m} \cdot (h_{in} - h_{out})$
	$\eta_{turbine} = (h_{in} - h_{out}) / (h_{in} - h_{out,is})$
Compressor	$W = \dot{m} \cdot (h_{out} - h_{in})$
	$\eta_{compressor} = (h_{out,is} - h_{in}) / (h_{out} - h_{in})$
Heat exchanger	$Q = \dot{m} \cdot (h_{out} - h_{in})$

For the heat exchanger model, in order to avoid internal pinch problem, discretized analysis is done for all the heat exchangers in the cycle. This analysis assumes that all the heat exchangers are counter-flow type. It gives the temperature distribution along the flow path, which helps to detect pinch problem and to keep the minimum pinch respect the pinch constraint in Table 2.

2. TES utilization

The TES utilization τ is defined as a ratio between utilized temperature range and allowed operation temperature range of the TES medium:

$$\tau = \frac{T_{upper}^{MS} - T_{lower}^{MS}}{T_{\max}^{MS} - T_{\min}^{MS}}$$

The allowed TES operation temperature range is defined based on the physical property of TES medium. For the commercially available Solar Salt currently used in CSP power plant, the allowed TES operation temperature range is between 290 ℃ and 565 ℃. Therefore, if in a certain TES design, the Solar Salt leaves the hot storage tank at 500 ℃ and enters the cold storage tank at 300 ℃, the TES utilization ratio, based on the definition above, is (500 ℃ – 300 ℃) / (565 ℃ – 290 ℃) = 72.73%. TES utilization ratio could also be defined based on enthalpy, with no major impact on the conclusions obtained in this study.

3. Specific Power Output

The specific power output w is defined as the power output that could be generated from a specific mass of thermal storage:

$$w = \frac{P \cdot t_{storage}}{m_{storage}}$$

Where $m_{storage}$ is TES storage molten salt amount in mass, $t_{storage}$ is TES storage hour, P is cycle net power.

4. Efficiency

The efficiency η definition here does not take into account the auxiliary consumption or mechanical losses in the turbo-machineries:

$$\eta = \frac{\sum W_{turbine} - \sum W_{compressor}}{\sum Q_{in}}$$

Where $W_{turbine}$ is the turbine output power, $W_{compressor}$ is the compressor power consumption, Q_{in} is the heat duty of molten salt/CO2 heat exchanger.

5. Cycle optimization

The algorithm used for cycle optimization is generalized reduced gradient method, together with stochastic initialization in order to avoid local optimum problem. For cycle optimization, the objective is to maximize the specific power output w while keeping the required TES utilization. The variables $\vec{X}$ to be optimized are summarized in Table 4.

Then the optimization problem can be expressed as:

DOI: 10.17185/duepublico/48879

Table 4
Governing equations for main equipment

Cycle	Variables to be optimized $\vec{X}$ + (T_{upper}^{MS}, $T_{tb,in}$, $T_{LTR,hot,out}$, p_{lower}, p_{upper}, $\dot{m}$)
RG	-
RG-IC	p_{IC}
RG-PH	$\tau_{PH,split}$, $T_{HTR,hot,out}$
RG-RH	$\tau_{RH,split}^{MS}$, T_{RH}, p_{RH}
RC	$\tau_{RC,split}$, $T_{HTR,hot,out}$
RC-IC	$\tau_{RC,split}$, $T_{HTR,hot,out}$, p_{IC}
RC-PH	$\tau_{PH,split}$, $T_{HTR,hot,out}$, $\tau_{PH,split}$
RC-RH	$\tau_{RC,split}$, $T_{HTR,hot,out}$, $\tau_{RH,split}^{MS}$, p_{RH}, T_{RH}
PC	$T_{HTR,hot,out}$, CR_{PC}
PC-IC	$T_{HTR,hot,out}$, CR_{PC}, p_{IC}
PC-PH	$T_{HTR,hot,out}$, CR_{PC},$\tau_{PH,split}$
PC-RH	$T_{HTR,hot,out}$, CR_{PC}, $\tau_{RH,split}^{MS}$, p_{RH}, T_{RH}
PartC	CR_{PC}, $\tau_{PC,out,split}$, $T_{HTR,hot,out}$
PartC-IC	CR_{PC}, $\tau_{PC,out,split}$, $T_{HTR,hot,out}$, p_{IC}
PartC-PH	CR_{PC}, $\tau_{PC,out,split}$, $T_{HTR,hot,out}$, $\tau_{PH,split}$
PartC-RH	CR_{PC}, $\tau_{PC,out,split}$, $T_{HTR,hot,out}$, $\tau_{RH,split}^{MS}$, p_{RH}, T_{RH}

$$Max.\ w\left(\vec{X}\right)$$

Subject to

$$\begin{cases} T_{upper}^{MS} \le T_{\max}^{MS} \\ T_{lower}^{MS} \ge T_{\min}^{MS} \\ \tau_{TES} = \tau_{given} \\ \forall\ x \in heat\ exchanger,\ \Delta T_x \ge \Delta T_{\min} \\ p_{upper} \le p_{\max} \\ \forall\ \tau,\ 1 \ge \tau \ge 0 \\ \forall\ CR,\ CR \ge 1 \end{cases}$$

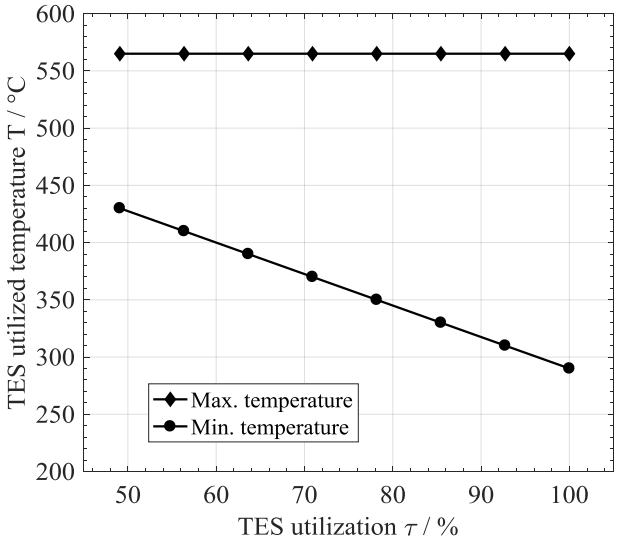

Figure 1: Effect of TES utilization on optimized TES utilized temperature range

RESULT AND DISCUSSION

The optimization is done case by case and each optimization case is defined by cycle layout and TES utilization. The objective of optimization for every case is to maximize the power output from a specific amount of TES medium.

Figure 1 shows the final TES utilized temperature range given by the optimization for all the studied cases. The optimization results show that, for every cycle layout and every TES utilization, the maximum utilized temperature is always equal to the maximum allowable temperature, i.e. 565 ℃ for Solar Salt. This is not a surprising result, because for a thermodynamic cycle which transforms thermal energy into mechanical energy, it is always more favorable to use high-grade heat in order to maximize the cycle efficiency. Besides, high-temperature molten salt has a higher specific heat capacity than that of low-temperature molten salt. This is another reason that it is more advantageous to use high temperature molten salt in order to maximize the power output from molten salt.

Figure 2 shows that, for the fundamental cycles, the specific power output decreases monotonically when TES utilization decreases. The specific power output reaches its maximum at 100% TES utilization. Considering that the power output is the product of cycle efficiency and thermal power input into the cycle, the results means that the cycle efficiency gain due to lower TES utilization and higher grade of heat from TES is not sufficient to compensate the loss of TES utilization potential. A higher TES utilization results in a smaller TES system but a lower cycle efficiency of power block, which leads to a bigger solar field. The TES utilization is also closely related to the solar receiver efficiency which has an important impact on solar field. Therefore, TES utilization is an important factor to be optimized when integrating SCO_2 cycle with CSP.

Figure 3 shows the evolution of optimized cycle efficiency with respect to the TES utilization. With the decrease of TES utilization, for each cycle, the cycle efficiency increases

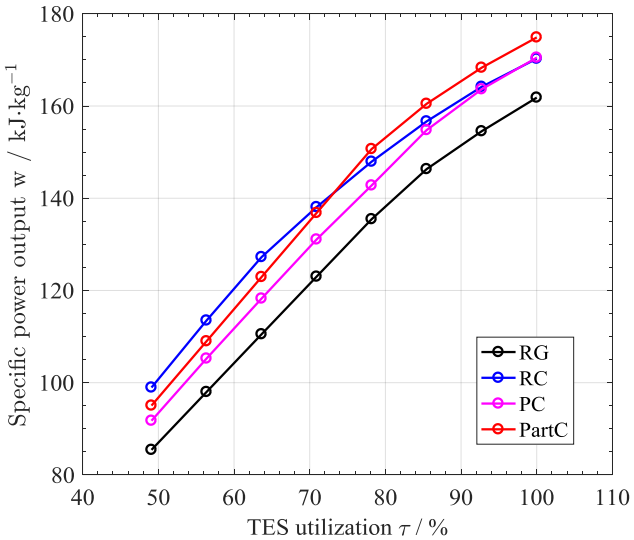

Figure 2: Effect of TES utilization on specific power output

DOI: 10.17185/duepublico/48879

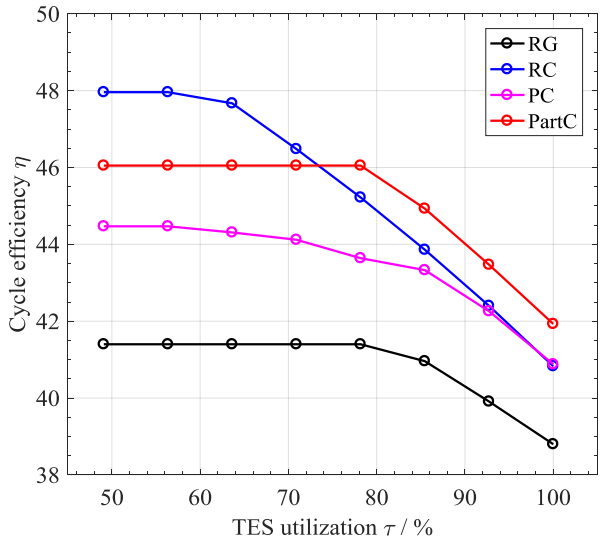

Figure 3: Effect of TES utilization on cycle efficiency for fundamental cycles

monotonically, mainly due to higher TIT temperature resulting from higher average heat source temperature. However, in general, except for reheating cycles, this trend could not be continued when it reaches its efficiency limit. The existence of this limit mainly comes from the fact that the TIT temperature could not be further increased any more when it reaches the temperature limit set by the heat source maximum temperature and the minimum pinch temperature allowed in the heat exchanger between heat source and CO_2. For reheating cycles, there are two turbines, one high-pressure turbine and one low-pressure turbine, with the same mass flow rate. As a result, there are two TITs to be maximized to the temperature limit, which leads to higher requirement on the heat source quality.

Table 5
Comparison between RG-FO and RG-PO cases (All extensive values are expressed as a ratio to that of RG-FO case)

		RG-FO	RG-PO
TIT	℃	504.23	560.00
TOT	℃	374.63	407.60
Pressure ratio	-	3.06	3.58
Cycle min. pressure	Bar	81.74	69.75
MCOT	℃	78.43	135.76
LTR UA	kW/℃	1.00	0.16
MH UA	kW/℃	1.00	4.47
Cooler UA	kW/℃	1.00	1.12
LTR heat duty	MW	1.00	0.52
MC work	MW	1.00	1.56
Turbine work	MW	1.00	0.97
MH heat duty	MW	1.00	1.00
Efficiency	%	38.80	31.30

Alternatively speaking, the efficiency limit of reheating cycle comes with a much lower TES utilization.

It is interesting to observe in Figure 4 that for high TES utilization level, TIT does not reach its upper limit to have the best cycle efficiency. Alternatively speaking, if TIT is set to its upper limit for high TES utilization, the cycle efficiency cannot reach its optimum. In order to keep TIT to its upper limit and reach a high TES utilization level, based on the general recuperation cycle layout, it requires the turbine to have a larger expansion ratio, then to have a larger temperature reduction through the turbine in order to have a better match with the TES low-end temperature. This makes the compressors have a higher compressor ratio and brings an extra constraint on the optimization of compressor operation condition, which results in higher compression energy consumption, and consequently, lower efficiency.

For RG cycle, a comparison for 100% TES utilization is shown in Table 5 between the full optimization case (RG-FO) and the partial optimization case (RG-PO). In the FO case, all the variables in Table 4 are optimized by the solver, but in the

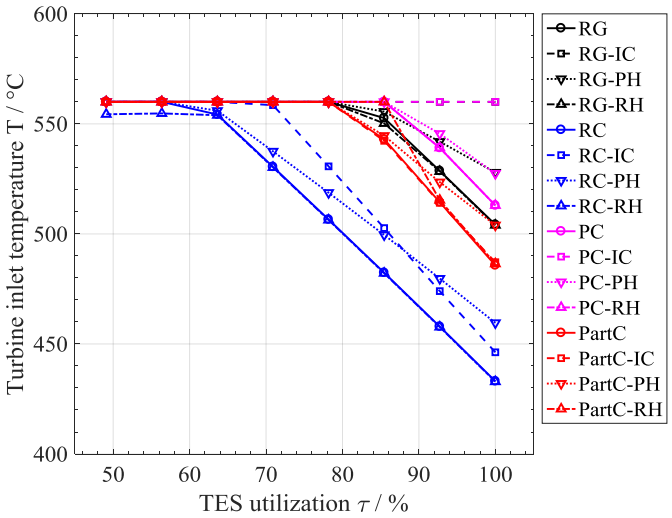

Figure 4: Effect of TES utilization on turbine inlet temperature

PO case, all are optimized except for TIT and TIT is set to be equal to the upper limit, i.e. 560 ℃ in this study. The final PO result shows that the cycle minimum pressure is optimized to be 69.75 bar. As a consequence, the main compressor has a higher compressor ratio of 3.58 and 56% higher compression work. This is the main reason that even with a higher TIT, the efficiency is only 31.30%, much lower than the FO case where the efficiency is 38.80%.

Among the four fundamental cycles, RG cycle, as the reference cycle, gives the lowest efficiency in the studied TES utilization range. RG gives efficiency of 38.80% at 100% TES utilization and the efficiency increases with the decrease of TES utilization and finally reach the highest efficiency of 41.40%. With pre-compression to solve the pinch problem in the recuperator, compared to RG cycle, PC cycle improves

DOI: 10.17185/duepublico/48879

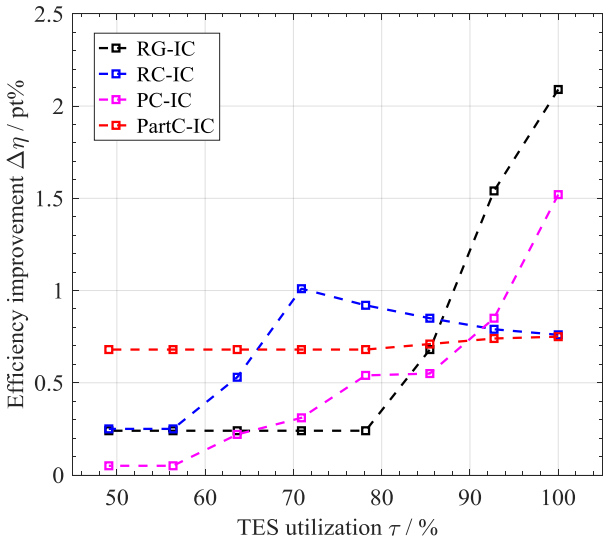

Figure 5: Effect of TES utilization on intercooling efficiency improvement effectiveness

significantly the efficiency, compared to RG cycle, +2 pt% at 100% TES utilization and +3 pt% at 49% TES utilization. RC cycle deals with the pinch problem by flow splitting. Comparing the optimization result of PC and RC cycle given in Figure 3, it is clear that flow splitting in RC cycle, in general, is a more efficient way to deal with this problem, which helps the cycle to recuperate better the exhaust heat from turbine outlet flow, especially in the region of low TES utilization. At 49% TES utilization, RC reaches the highest efficiency of 47.96%, +3.5% higher than PC cycle. PartC cycle outperforms the other three fundamental cycles in the region of high TES utilization. Compared to RC cycle, the efficiency improvement mainly comes from the fact that extra cooling at the outlet of low-temperature recuperator helps to increase the TIT while keeping the TES utilization at a high level. But high TIT and high TES utilization leads to a high compression ratio, which makes the cycle minimum pressure close to 60 bar.

This low pressure could make the operation of compressor very difficult. However, this extra cooling becomes a constraint for exhaust heat recuperation when TES utilization ratio is below 73%, therefore, RC cycle efficiency becomes higher than that of PartC cycle. When reaching the region of convergence, PartC achieves its highest efficiency of 46.05%, near -2% lower than RC cycle efficiency at convergence.

As shown by Figure 5, combining IC with the fundamental cycles could generally improves efficiency, especially at the high TES utilization region, because intercooling helps to reduce compressor outlet temperature, then better use the low-grade heat from heat source. In the meantime, as shown in Figure 4, it helps to reach a higher TIT with the same TES utilization. At the low TES utilization region, IC also helps on the efficiency improvement but less evidently. Since the intercooling is done on the compressor that operates on the whole flow for RG cycle and PC cycle, IC helps more significantly to increase the efficiency, by +2.09 pt% at 100% TES utilization for RG cycle and by +1.52 pt% for PC cycle. For RC cycle, the highest IC improvement occurs at 71% TES utilization, near +1 pt%. The impact of IC on PartC cycle is almost constant for the studied range of TES utilization, with a maximum efficiency improvement of +0.75 pt% at 100% TES utilization.

As shown by Figure 6, combining PH with the fundamental cycles could improves efficiency, but only at the high TES utilization region. Because PH is designed to split part of the low-temperature flow during recuperation to recover the low-grade heat from heat source, it is not surprising that it could achieve a higher efficiency at high TES utilization. At low TES utilization, there is no lower grade heat that could match the temperature profile during recuperation, therefore, PH is not useful any more. PH helps significantly RC cycle to improve efficiency because RC cycle is not adapted to utilize low-grade heat. PartC cycle, with extra cooling before compression, compared to PartC cycle, could behave better with low-grade heat, therefore, the impact of PH on PartC is less evident. PH, with the flow splitting between recuperator, provide an

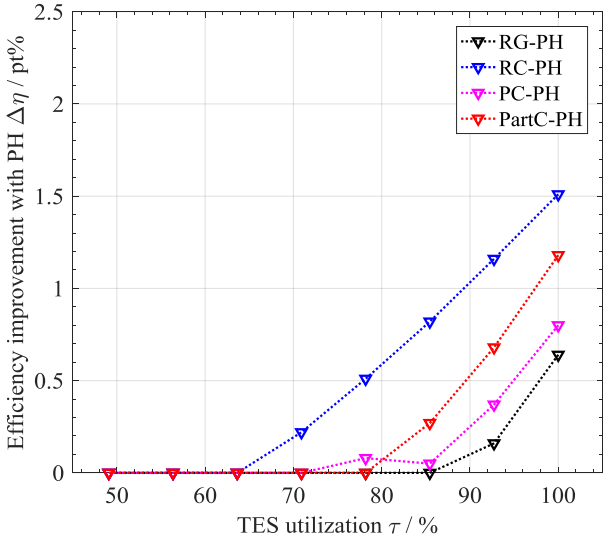

Figure 6: Effect of TES utilization on intercooling efficiency improvement effectiveness

additional approach for PC and RG cycle to improve the recuperation, therefore, improvement is also observed for these cycles.

As shown by Figure 7, combining RH with the fundamental cycles could improves efficiency, but only at the low TES utilization region, which is opposite to the effect of IC and PH. For RH, the molten salt flow is divided into two parts to heat the whole CO_2 flow at different locations. At high TES utilization, without additional measure, any effort to divide the molten salt into two is difficult for efficiency improvement because this leads to mismatch between the mass flow of molten salt and that of CO_2. With this mismatch, a higher CO_2 inlet temperature or a smaller CO_2 mass flow is required in order to achieve a better

DOI: 10.17185/duepublico/48879

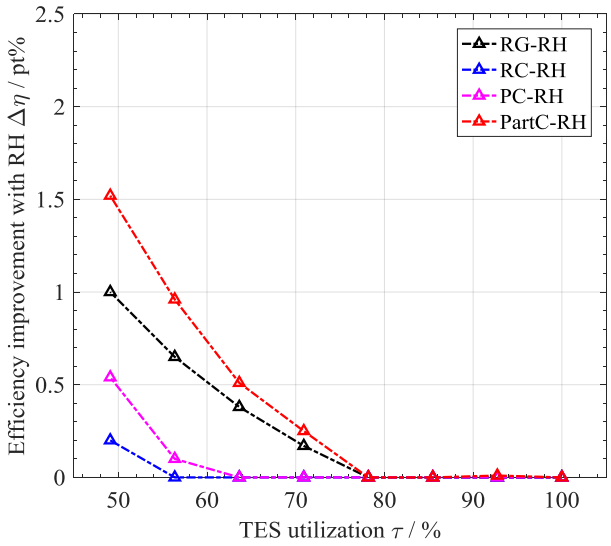

Figure 7: Effect of TES utilization on reheating efficiency improvement effectiveness

main heater effectiveness. In the first case where a higher main heater inlet temperature is required, it is necessary to have a high TOT, which has a negative impact on turbine power output then leads to efficiency loss. Besides, this is also limited by the high TES utilization requirement. In the second case where CO_2 mass flow should be reduced, in general, in order to still keep power output at a high level, it is necessary to reach a high cycle pressure ratio. Finally, the optimization is a balance between efficiency gain due to reheating and efficiency loss due to the necessity to keep a high TOT and a high pressure ratio. According to the results, the efficiency gain due to reheating dominates the trends when TES utilization is lower than 80%. Therefore, generally, RH is a measure to better use the high-grade heat when available. PartC cycle, due to the existence of extra cooling, it achieves a high cycle pressure ratio and a smaller CO_2 mass flow rate, then it is able to implement RH in an effective way and it helps the most for PartC cycle, because PartC cycle provides a more suitable structure to match the requirement of RH. RC cycle is more suitable for high-grade heat source. Because by flow splitting, it could achieve very effective recuperation of turbine exhaust heat, it tends to reach the highest possible main heater CO_2 inlet temperature. But for high TES utilization, this trend is limited by the molten salt outlet temperature. RH intensifies the same trends as RC cycle, with the constraint of TES utilization, it is not useful until very low TES utilization. According to the result, when TES utilization becomes smaller than 56%, RH becomes effective to the efficiency improvement. RG cycle is the basic cycle with poor recuperation and poor efficiency. Due to the poor recuperation, the main heater inlet temperature cannot be heated to the limit set by the turbine outlet temperature and pinch, therefore, there is still efficiency improvement margin for RH to be effective in RG cycle. In terms of recuperation effectiveness, PC cycle is between RG and RC cycle, therefore, in average, the impact of RH on PC is between these two cycles.

Among all the cycle studies, as shown by Figure 8, for TES utilization between 100% and 93%, i.e. molten salt exhaust temperature between 290 ℃ and 310 ℃, PartC-PH gives the highest efficiency from 43.11% to 44.16%. For TES utilization between 93% and 75%, i.e. molten salt exhaust temperature between 310 ℃ and 359 ℃, PartC-IC gives the highest efficiency from 44.16% to 46.73%. For TES utilization between 75% and 49%, i.e. molten salt exhaust temperature between 359 ℃ and 430 ℃, RC-IC gives the highest efficiency from 46.73% to 48.21%. For TES utilization below 49%, it is observed that RC-RH cycle efficiency continues to increase with the decrease of TES utilization. When TES utilization reaches approximately 45%, the RC-RH starts to outperform all the other cycles. Solar Salt is allowed to operate between 565 ℃ and 290 ℃, but with less than 50% TES utilization, only half of the thermal storage potential is used, which means, compared to full utilization, TES system needs two times molten salt, much bigger molten salt storage tank and auxiliary systems, as a result, much larger investment. In this case, even with a higher cycle efficiency, there is no guarantee that it will be an optimal cycle for CSP project.

CONCLUSION

In this study, four fundamental SCO_2 cycles, together with twelve cycle derivatives are modeled, optimized and compared in the context of integrating SCO_2 cycle with high-temperature CSP technology which is currently available for industry, i.e. CSP with Solar Salt tower. Based on this comparison, the study focuses on understanding the cycle performance behaviors with different TES utilization. Main conclusions are drawn as follows:

1) It is always more favorable to use higher-temperature molten salt when available.
2) Lower TES utilization, i.e. higher molten salt exhaust temperature, helps to reach higher cycle thermal efficiency, but at the cost of reducing specific power output of thermal storage system. Alternatively speaking, with lower TES utilization, for the same size of thermal storage system, it can only produce less electricity, even with a higher cycle efficiency.
3) For high TES utilization, it is not always optimal for TIT to reach its upper temperature limit set by the maximum molten salt temperature.
4) Intercooling can help to improve cycle efficiency, and in general, it is more effective at high TES utilization.
5) Preheating can help to improve cycle efficiency, but only at high TES utilization. For the considered cycles in this study, when TES utilization is lower than 64%, preheating could not help any more for efficiency improvement.
6) Reheating can help to improve cycle efficiency, but only at low TES utilization. For PartC cycle and RG cycle, it starts to be effective when TES utilization is lower than 78%. For PC cycle, it starts to be effective

DOI: 10.17185/duepublico/48879

when TES utilization is lower than 64%. For RC cycle, it starts to be effective when TES utilization is lower than 56%.

7) Among all the considered cycles, in terms of efficiency, PartC-PH cycle is optimal for TES utilization between 100% and 93%; ParC-IC cycle is optimal for TES utilization between 93% and 75%; RC-IC cycle is optimal for TES utilization between 75% and 49%.

In a conclusion, TES utilization is an important factor when integrating SCO_2 cycle with CSP, because it serves as the key interface parameter between solar field, TES and power block. As shown by this study, it has an important impact on the selection of SCO_2 cycle for CSP. It is also evident that TES utilization, together with other key parameters such as storage hour and design net power output, directly determine the size of TES system. In the meanwhile, TES utilization influences directly the receiver thermal loss and indirectly the size of solar field via thermal cycle efficiency. Therefore, keeping TES utilization as a factor to be optimized, a global study that takes solar field and TES system into account should be further done to analyze the performance of SCO_2 cycle.

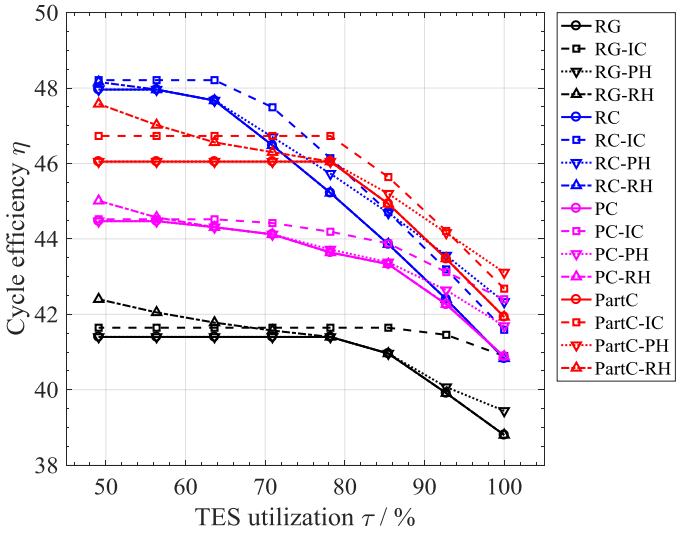

Figure 8: Effect of TES utilization on reheating efficiency improvement effectiveness

NOMENCLATURE

Symbols	
CR	compression ratio
P	power (MW)
p	pressure (MPa)
Q	heat duty (MW)
T	temperature (℃)
W	turbine/compressor work (MW)
Greek symbols	
η	efficiency
τ	split ratio
Abbreviations	
AC	auxiliary compressor
C	cooler
CO_2	Cabon dioxide
CSP	concentrated solar power
FO	full optimization
HTR	high temperature recuperator
IC	intercooling
LCOE	Levelized cost of electricity
LTR	low-temperature recuperator
MC	main compressor
MH	main heater
PartC	partial cooling
PC	pre-compression / pre-compressor
PH	Preheating / preheater
PO	partial optimization
RC	recompression
RG	regenerative
RH	reheating
SCO_2	supercritical CO_2
TES	thermal energy storage
TIT	turbine inlet temperature
TOT	turbine outlet temperature
Subscripts/superscripts	
cold	cold side flow of heat exchanger
Hot	hot side flow of heat exchanger
in	inlet flow
MS	molten salt
out	outlet flow
split	flow split
tb	turbine

REFERENCES

[1] Liu S, Bie Z, Lin J, Wang X. Curtailment of renewable energy in Northwest China and market-based solutions. Energy Policy 2018;123:494–502. doi:10.1016/j.enpol.2018.09.007.

[2] Turchi CS. Supercritical CO2 for Application in Concentrating Solar Power Systems. Supercrit. CO2 power cycle Symp. Troy, New York, 2009.

[3] Glatzmaier GC, Turchi CS. Supercritical CO2 as a Heat Transfer and Power Cycle Fluid for CSP Systems. ASME Int. Conf. energy Sustain. San Fr., 2009. doi:10.1115/es2009-90332.

[4] Ma Z, Turchi CS. Advanced Supercritical Carbon Dioxide Power Cycle Configurations for Use in Concentrating Solar Power Systems. Supercrit. CO2 power cycle Symp. Boulder, Color., 2011.

[5] Turchi CS, Ma Z, Dyreby J. Supercritical Carbon Dioxide Power Cycle Configurations for Use in Concentrating Solar Power Systems. ASME Turbo Expo, Copenhagen, Denmark, 2012. doi:10.1115/GT2012-68932.

[6] Neises T, Turchi CS. Supercritical carbon dioxide power cycle design and configuration optimization to minimize levelized cost of energy of molten salt power

DOI: 10.17185/duepublico/48879

towers operating at 650°C. Sol Energy 2019;181:27–36. doi:10.1016/j.solener.2019.01.078.
[7] Feher EG. The supercritical thermodynamic power cycle. Energy Convers 1968;8:85–90. doi:10.1016/0013-7480(68)90105-8.
[8] Angelino G. Real Gas Effects in Carbon Dioxide Cycles. ASME Gas turbine Conf. Prod. show, Cleveland, Ohio, 1969. doi:10.1115/69-gt-102.
[9] Ahn Y, Bae SJ, Kim M, Cho SK, Baik S, Lee JI, et al. Review of supercritical CO 2 power cycle technology and current status of research and development. Nucl Eng Technol 2015;47:647–61. doi:10.1016/j.net.2015.06.009.
[10] Dostal V. A Supercritical Carbon Dioxide Cycle for Next Generation Nuclear Reactors. Massachusetts Institute of Technology, 2004.
[11] Angelino G. Perspectives for the Liquid Phase Compression Gas Turbine. J Eng Gas Turbines Power 1967;89:229–36. doi:10.1115/1.3616657.
[12] Angelino G. Carbon dioxide condensation cycles for power production. J Eng Gas Turbines Power 1968;90:287–95. doi:10.1115/1.3609190.
[13] Yamaguchi H, Zhang XR, Fujima K, Enomoto M, Sawada N. Solar energy powered Rankine cycle using supercritical CO2. Appl Therm Eng 2006;26:2345–54. doi:10.1016/j.applthermaleng.2006.02.029.
[14] Zhang XR, Yamaguchi H, Uneno D. Experimental study on the performance of solar Rankine system using supercritical CO2. Renew Energy 2007;32:2617. doi:10.1016/j.renene.2007.01.003.
[15] Zhang XR, Yamaguchi H. An experimental study on evacuated tube solar collector using supercritical CO2. Appl Therm Eng 2008;28:1225–33. doi:10.1016/j.applthermaleng.2007.07.013.
[16] Neises T, Turchi CS. A comparison of supercritical carbon dioxide power cycle configurations with an emphasis on CSP applications. Energy Procedia 2013;49:1187–96. doi:10.1016/j.egypro.2014.03.128.
[17] Le Moullec Y. Conceptual study of a high efficiency coal-fired power plant with CO2 capture using a supercritical CO2 Brayton cycle. Energy 2013;49:32–46. doi:10.1016/j.energy.2012.10.022.
[18] Mecheri M, Le Moullec Y. Supercritical CO2 Brayton cycles for coal-fired power plants. Energy 2016;103:758–71. doi:10.1016/j.energy.2016.02.111.
[19] Xu J, Sun E, Li M, Liu H, Zhu B. Key issues and solution strategies for supercritical carbon dioxide coal fired power plant. Energy 2018;157:227–46. doi:10.1016/j.energy.2018.05.162.
[20] Lehar MA, Michelassi V. System and method for recovery of waste heat from dual heat sources. U.S. Patent No. 9038391, 2012.
[21] Timothy J. Held. Supercritical CO2 cycles for gas turbine combined power plants. Power Gener. Int. Las Vegas,Nevada, 2014.
[22] Huck P, Freund S, Lehar M, Peter M. Performance comparison of supercritical CO2 versus steam bottoming cycles for gas turbine combined cycle applications. 5th Int Symp - SCO2 Power Cycles2 2016. doi:10.1017/CBO9781107415324.004.
[23] Chacartegui R, Muñoz De Escalona JM, Sánchez D, Monje B, Sánchez T. Alternative cycles based on carbon dioxide for central receiver solar power plants. Appl. Therm. Eng., 2011. doi:10.1016/j.applthermaleng.2010.11.008.
[24] Dunham MT, Iverson BD. High-efficiency thermodynamic power cycles for concentrated solar power systems. Renew Sustain Energy Rev 2014;30:758–70. doi:10.1016/j.rser.2013.11.010.
[25] Cheang VT, Hedderwick RA, McGregor C. Benchmarking supercritical carbon dioxide cycles against steam Rankine cycles for Concentrated Solar Power. Sol Energy 2015;113:199–211. doi:10.1016/j.solener.2014.12.016.
[26] Al-Sulaiman FA, Atif M. Performance comparison of different supercritical carbon dioxide Brayton cycles integrated with a solar power tower. Energy 2015;82:61–71. doi:10.1016/j.energy.2014.12.070.
[27] Wang K, He YL, Zhu HH. Integration between supercritical CO2 Brayton cycles and molten salt solar power towers: A review and a comprehensive comparison of different cycle layouts. Appl Energy 2017;195:819–36. doi:10.1016/j.apenergy.2017.03.099.
[28] Wang K, Li MJ, Guo JQ, Li P, Liu Z Bin. A systematic comparison of different S-CO2 Brayton cycle layouts based on multi-objective optimization for applications in solar power tower plants. Appl Energy 2018;212:109–21. doi:10.1016/j.apenergy.2017.12.031.
[29] Guo J-Q, Li M-J, Xu J-L. Performance comparison of SPT systems integrated with various supercritical CO2-based mixture Brayton cycles based on multi-objective optimization. Energy Procedia 2019;158:1823–8. doi:10.1016/j.egypro.2019.01.427.

DOI: 10.17185/duepublico/48879

ANNEX A

FUNDAMENTAL SCO_2 CYCLES AND THEIR DERIVATIVES

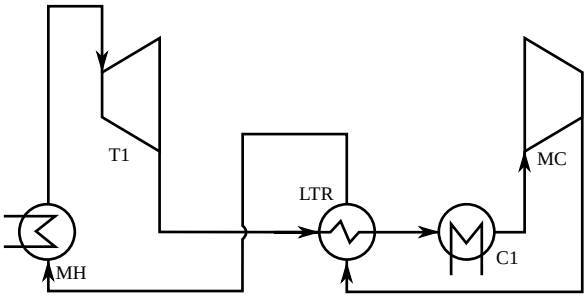

Figure 9: Regenerative (RG) cycle

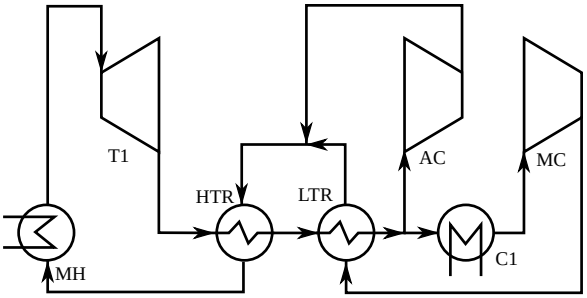

Figure 13: Recompression (RC) cycle

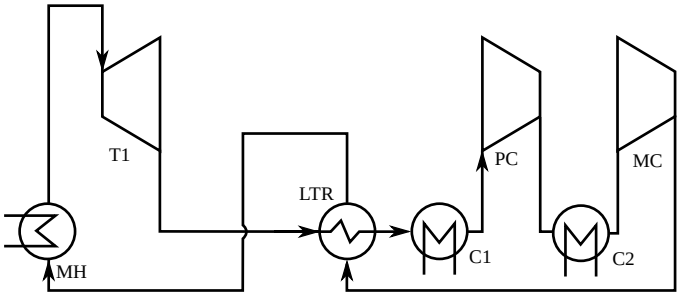

Figure 10: Regenerative (RG) cycle with intercooling (IC)

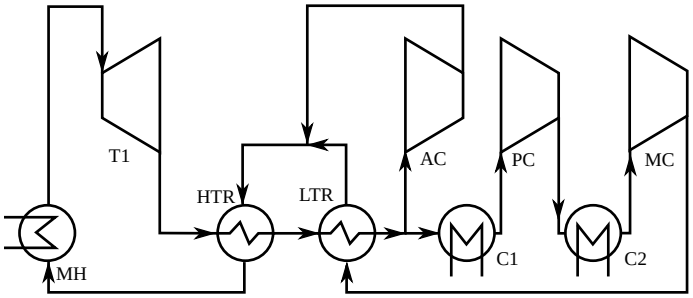

Figure 14: Recompression (RC) cycle with intercooling (IC)

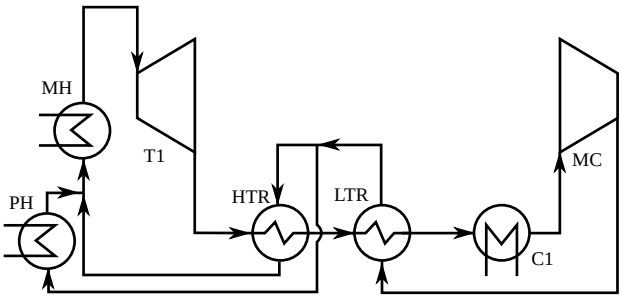

Figure 11: Regenerative (RG) cycle with preheating (PH)

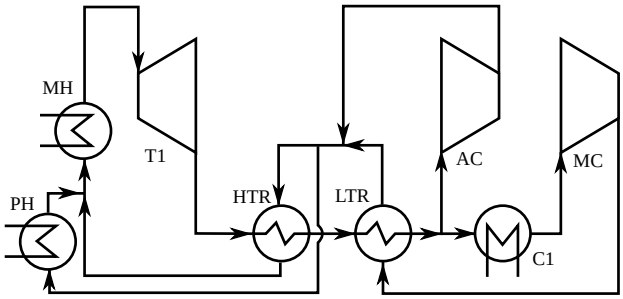

Figure 15: Recompression (RC) cycle with preheating (PH)

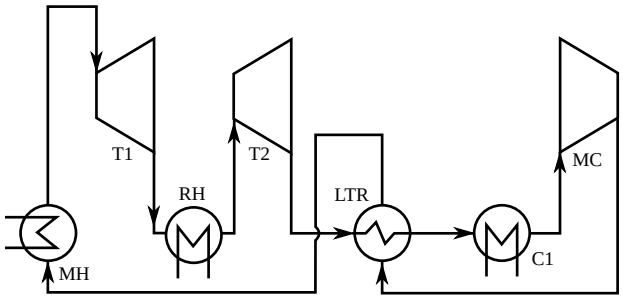

Figure 12: Regenerative (RG) cycle with reheating (RH)

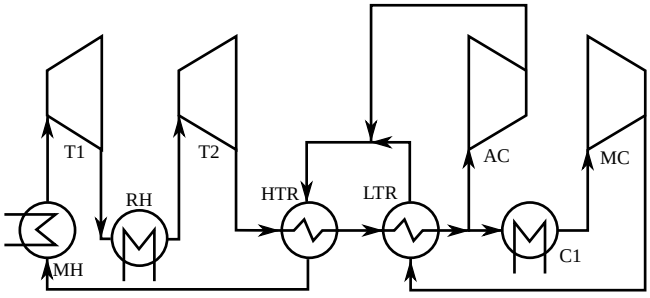

Figure 16: Recompression (RC) cycle with reheating (RH)

DOI: 10.17185/duepublico/48879

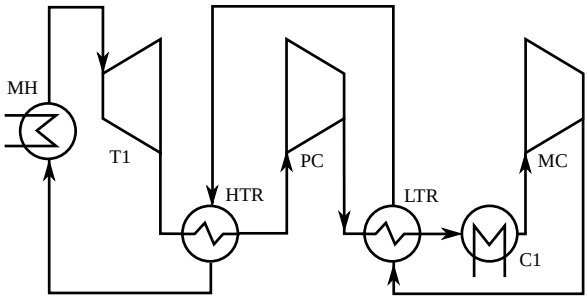

Figure 17: Pre-compression (PC) cycle

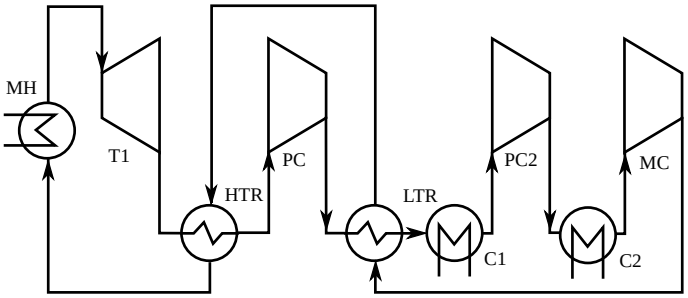

Figure 18: Pre-compression (PC) cycle with intercooling (IC)

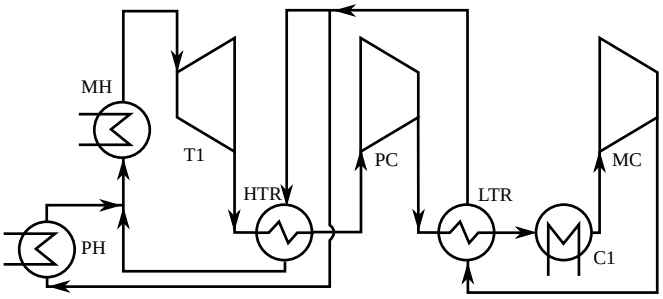

Figure 19: Pre-compression (PC) cycle with preheating (PH)

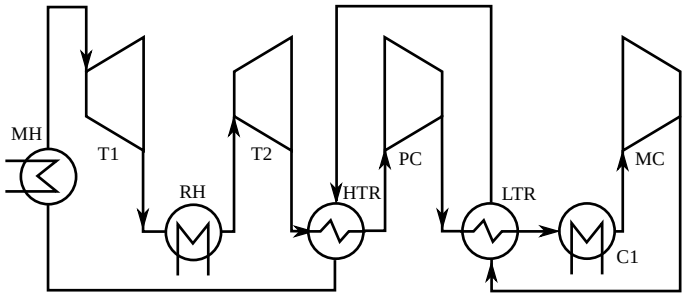

Figure 20: Pre-compression (PC) cycle with reheating (RH)

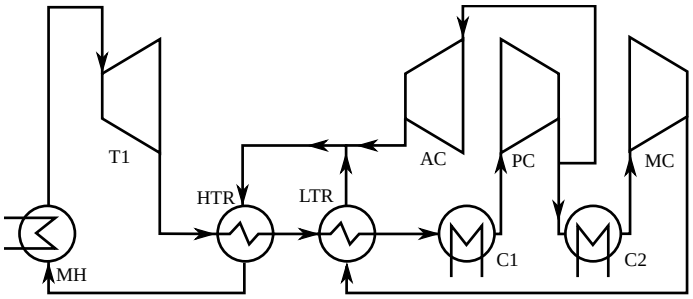

Figure 21: Partial cooling (PartC) cycle

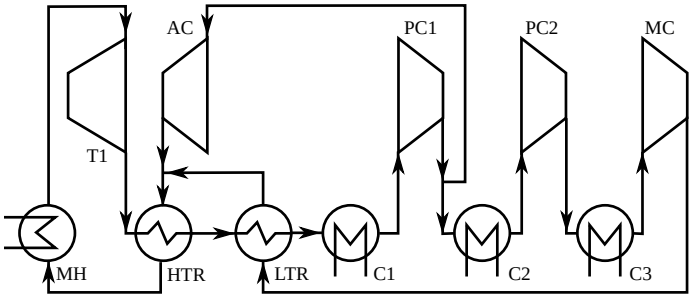

Figure 22: Partial cooling (PartC) cycle with intercooling (IC)

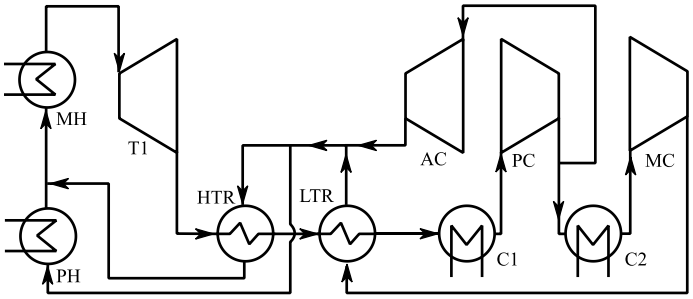

Figure 23: Partial cooling (PartC) cycle with preheating (PH)

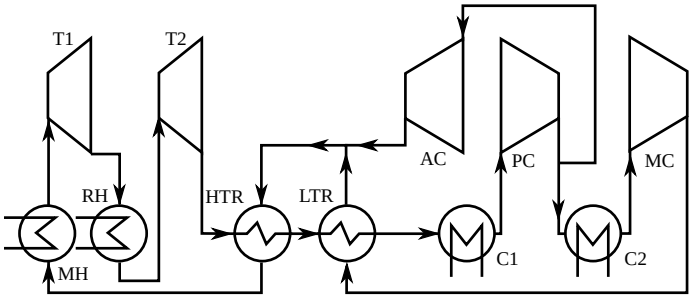

Figure 24: Partial cooling (PartC) cycle with reheating (RH)

DOI: 10.17185/duepublico/48879

DOI: 10.17185/duepublico/48904
URN: urn:nbn:de:hbz:464-20191002-165915-2